

Northwest Sumatra and Offshore Islands Field Survey after the December 2004 Indian Ocean Tsunami

Bruce E. Jaffe,^{a)} Jose C. Borrero,^{b)} Gegar S. Prasetya,^{c)} Robert Peters,^{a)} Brian McAdoo,^{d)} Guy Gelfenbaum,^{e)} Robert Morton,^{f)} Peter Ruggiero,^{e)} Bretwood Higman,^{g)} Lori Dengler,^{h)} M.EERI, Rahman Hidayat,ⁱ⁾ Ettiene Kingsley,^{j)} Widjo Kongko,ⁱ⁾ Lukijanto,^{c)} Andrew Moore,^{k)} Vasily Titov,^{l)} and Eko Yulianto^{m)}

An International Tsunami Survey Team (ITST) conducted field surveys of tsunami effects on the west coast of northern and central Sumatra and offshore islands 3–4 months after the 26 December 2004 tsunami. The study sites spanned 800 km of coastline from Breuh Island north of Banda Aceh to the Batu Islands, and included 22 sites in Aceh province in Sumatra and on Simeulue Island, Nias Island, the Banyak Islands, and the Batu Islands. Tsunami runup, elevation, flow depth, inundation distance, sedimentary characteristics of deposits, near-shore bathymetry, and vertical land movement (subsidence and uplift) were studied. The maximum tsunami elevations were greater than 16 m, and the maximum tsunami flow depths were greater than 13 m at all sites studied along 135 km of coastline in northwestern Sumatra. Tsunami flow depths were as much as 10 m at 1,500 m inland. Extensive tsunami deposits, primarily composed of sand and typically 5–20 cm thick, were observed in northwestern Sumatra. [DOI: 10.1193/1.2207724]

INTRODUCTION

The Indian Ocean tsunami of 26 December 2004 caused widespread devastation and loss of life throughout the Indian Ocean basin and beyond. The tsunami was generated by a large earthquake ($M_w=9.0-9.3$) that ruptured a 1,200–1,300 km segment of inter-

^{a)} United States Geological Survey Pacific Science Center, 400 Natural Bridges Drive, Santa Cruz, CA 95060

^{b)} Department of Civil Engineering, University of Southern California, Los Angeles, CA 90089

^{c)} P3TISDA BPPT, Jl.MH.Thamrin 8 Jakarta, DKI Jaya, 10340, Indonesia

^{d)} Department of Geology, Vassar College, Poughkeepsie, NY 12601

^{e)} United States Geological Survey, 345 Middlefield Road MS-999, Menlo Park, CA 94025

^{f)} United States Geological Survey, Center for Coastal and Watershed Studies, 600 Fourth Street South, St. Petersburg, FL 33701-4846

^{g)} Department of Earth and Space Sciences, University of Washington, Seattle, WA 98195

^{h)} Geology Department, Humboldt State University, Arcata, CA 95521

ⁱ⁾ BPDP BPPT Jl. Grafika 2 Bulaksumur, Jogjakarta DI. Jogjakarta, 55281, Indonesia

^{j)} 600 Black Lake Blvd. SW, Apt.158, Olympia, WA 98502

^{k)} Department of Geology, Kent State University, Kent, OH 44242

^{l)} National Oceanic & Atmospheric Administration Pacific Marine Environmental Laboratory, 7600 Sand Point Way NE, Building 3, Seattle, WA 98115

^{m)} Indonesian Institute of Science (GEOTEK LIPI), Ji. Sangkuriang, Bandung 40135, Indonesia



Figure 1. Survey area, showing the epicenter of the 26 December earthquake and the interplate thrust fault, indicated by the sawtoothed line. This figure was modified from a USGS poster, “Sumatra-Andaman Islands Earthquake of 26 December 2004—Magnitude 9.0,” which can be accessed at <http://neic.usgs.gov/neis/poster/2004/20041226.html>.

plate megathrust extending from offshore northern Sumatra to the Andaman Islands (Lay et al. 2005, USGS 2005, Stein and Okal 2005) (Figure 1). The earthquake occurred at 07:58 local time in Indonesia (00:58 UTC). The tsunami arrived in northern Sumatra, the hardest-hit region, within 15–20 minutes after the earthquake. Fatalities from the tsunami and earthquake in Indonesia totaled 128,645, with more than 37,063 persons missing and 532,898 persons displaced (USAID 2005). Virtually all of the loss of life and damage is attributable to the tsunami.

The initial post-tsunami field survey in Indonesia was of northwest and northeast

Sumatra, including the hard-hit Banda Aceh area, and was conducted during the first week of January 2005 (Borrero 2005; Borrero 2006, this issue). Tsunami scientists from Indonesia, Japan, Turkey, Russia, and the United States conducted three additional surveys in January in northern Sumatra and the offshore islands (Tsuji et al. 2005a, Yalciner et al. 2005, Gusiakov 2005). The largest measured tsunami heights, which were at Lhoknga in northwest Sumatra, about 15 km southwest of Banda Aceh, were greater than 30 m (Tsuji et al. 2005a, Borrero 2005). The tsunami height decreased to about 15 m at Meulaboh (Yalciner et al. 2005), which is in northwestern Sumatra, about 175 km southeast of Banda Aceh. Tsunami heights of about 2 m were measured in Sibolga, a fishing port in a natural embayment about 500 km southwest of Banda Aceh. During the January surveys, most of the roads were impassable, resulting in large gaps in the field data collected.

To fill these data gaps, an International Tsunami Survey Team (ITST) consisting of 12 U.S. and 5 Indonesian scientists (the authors of this paper) formed to collect additional data on the 26 December 2004 tsunami. The ITST included experts in tsunami geology, tsunami hydrodynamics (tsunami propagation and inundation), tsunami hazard assessment, tsunami education, coastal geology and processes, bathymetry collection, and palynology. This ITST was different from previous ITSTs in that it had seven geologists, the greatest number of geologists in a post-tsunami survey ever. The composition of the ITST allowed collection of both tsunami water level and deposit data, including documentation of the deposits from the 26 December tsunami and reconnaissance for paleotsunami deposits. Coastal change data, including estimates of subsidence and uplift, and data on the adjustment of the coast to the new land levels were also collected.

The presurvey goals of the data collection effort were to (1) fill the data gaps of previous surveys in the measurements of tsunami elevation, flow depth, runup elevation, and inundation distances between Lhoknga (northern Sumatra) and Padang (southern Sumatra); (2) conduct detailed sedimentological investigations, including paleotsunami studies; (3) survey topography and near-shore bathymetry, filling a critical data void for tsunami propagation and inundation modeling; (4) investigate the effectiveness of previous tsunami education and hazard mitigation strategies; and (5) make additional estimates of coseismic subsidence and uplift from the 26 December earthquake.

To accomplish these goals, the ITST was divided into two groups that conducted surveys from 31 March to 22 April 2005, using a charter boat that served both as transportation and lodging. While the first group was assembling in Jakarta, Indonesia en route to the survey area on 28 March 2005, a magnitude 8.7 earthquake occurred on the adjacent megathrust segment to the south of the one that ruptured on 26 December 2004. A new, high-priority goal of documenting the tsunami created by this earthquake was added to the previous goals. This paper presents only the results of investigations of the 26 December tsunami. Initial observations of both the 26 December 2004 and 28 March 2005 tsunamis are posted at <http://walrus.wr.usgs.gov/news/reports.html>.

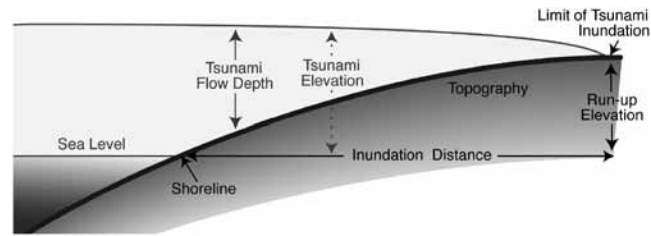


Figure 2. A tsunami inundating land, illustrating the terminology used in this paper.

FIELD METHODS

The ITST collected measurements in a manner similar to other post-tsunami field investigations (Dengler et al. 2003, Gelfenbaum and Jaffe 2003). Measurements were made primarily on shore-normal transects, although a considerable number of off-transect measurements were also made. Sites were chosen by using satellite imagery, information from surveys made in January 2005, and logistical considerations.

Tsunami water levels and topography were measured relative to sea level at the shore at the time of the survey via a laser rangefinder aimed at either a prism on top of a survey rod or a water level indicator (e.g., debris in a tree). Water elevations at all but the southernmost sites were corrected to the tidal level at 09:00 on 26 December 2004, which is approximately one hour after the earthquake, using tides calculated by Tsuji et al. (2005b). The one-hour delay was chosen because eyewitnesses near Banda Aceh reported that a later wave, not the first wave, was the largest and because eyewitness reports of the arrival time of the first wave varied from approximately 15 minutes near Banda Aceh to 30 minutes at Simeulue Island. The water level data we collected represent a combination of effects from all the waves in the wave train. The largest wave caused the maximum tsunami water level or greatly influenced it if multiple waves were additive. Hence, we corrected to our best estimate of the sea level at the arrival time of the largest wave. In practice, the choice of the tsunami arrival time used for tidal correction, except for the southern sites, does not introduce error greater than 0.2 m, because the tidal range is low (<1 m). For subsided regions, inland distances were referenced to the shoreline at the time of the survey. These distances have not been corrected to the pretsunami shoreline location, which is the most relevant distance for planning purposes and typically was farther seaward because of erosion during and after the tsunami. Distances in uplifted regions were referenced to the shoreline location before the earthquake and tsunami, which was detectable from field evidence.

The measured water levels included (1) runup elevation, which is the elevation at maximum inundation; (2) flow depth during the tsunami, which is the height of the tsunami above the ground; and (3) tsunami elevation, or the height above sea level, which is the sum of the flow depth and land elevation (Figure 2). The minimum flow depths during the tsunami were indicated by broken branches (Figure 3a) or stripped bark in trees, debris in trees, snapped trees, gouge marks in trees, impact marks on rock out-

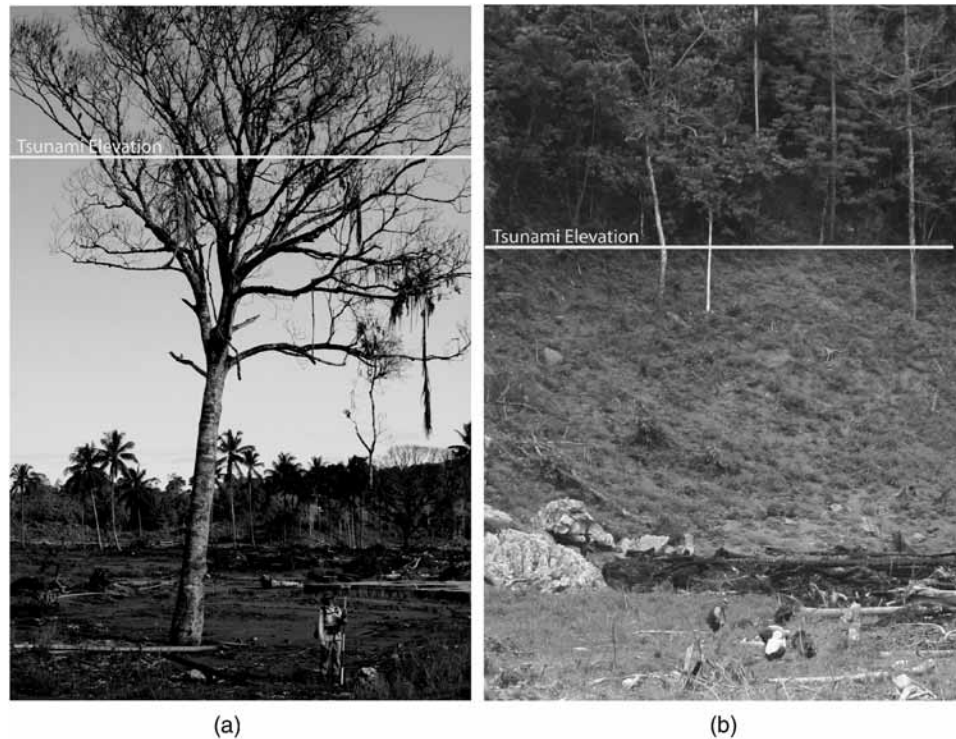


Figure 3. (a) Surveying the topographic profile in front of a large tree that survived the 26 December tsunami at Lhok Kruet, Sumatra. Note the branches high in the tree that were broken by the tsunami. The combination of broken branches and debris high in the tree, primarily palm fronds, indicate that the tsunami flow depth was 9.9 m at this location, which is approximately 275 m inland. (b) Trim line at Jantang at 19.7 m above sea level when the tsunami struck. Vegetation below the line was stripped by the tsunami and had begun to grow back. In the foreground, the team members examine a tsunami deposit (photos: B. Jaffe).

crops, and watermarks on buildings (rare along the sites on the west coast of Sumatra visited by this ITST, because nearly all the buildings were destroyed). Runup was indicated either by a wrack line of debris or a trim line, which is the level on a hill or cliff below which all vegetation was stripped by the tsunami (Figure 3b).

Flow directions were estimated in the field from the orientation of trees ripped up by the tsunami, aligned debris on the ground, preferential scour around buildings, toppled palm trees and building materials, debris wrapped around trees and structures, and bent vegetation. Bent vegetation within or at the base of tsunami deposits was also used to determine flow direction.

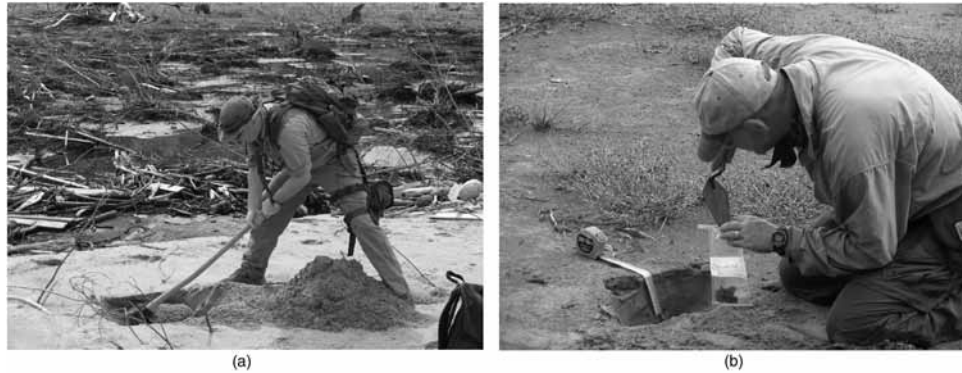


Figure 4. (a) Trenching at Jantang, Sumatra. This trench is in a berm that formed several months after the tsunami as the shoreline and the near-shore area adjusted to coseismic subsidence and erosion from the tsunami. The area landward of the trench was flooded because it had subsided during the 26 December earthquake (photo: A. Moore). (b) Collection of tsunami deposit samples for laboratory analyses of grain size (photo: B. Higman).

Tsunami deposits were examined in pits and trenches dug at intervals along a shore-normal transect and at selected off-transect locations (Figure 4a). The deposits were measured, photographed, and described in the field, and samples were taken for laboratory analyses. In the field, bulk samples of layers within the deposits were taken, and, at about a dozen locations, samples were taken at 0.5-cm or 1-cm intervals to document the fine-scale vertical variation of grain size in the deposit (Figure 4b). The goal of collecting these samples is to use them, in conjunction with field observations, photos, and peels, to develop relations between the tsunami flow and the deposit it leaves (e.g., the relations between flow speed and deposit characteristics).

At several sites, the ITST searched for paleotsunami deposits by taking push cores in environments with good preservation potential and by examining eroded channel banks and scarps near the shoreline (Figure 5a). Potential paleotsunami deposits were measured, photographed, and described in the field, and samples were taken for laboratory analyses.

Near-shore bathymetric data were collected at selected sites by using a simplified version of the coastal profiling system, as described by Ruggiero et al. (2005). A shallow-water echo sounder and GPS antenna were mounted to a stainless steel mast attached to the 25' skiff, the RV *Scarab*. HYPACK hydrographic surveying software from Coastal Oceanographics Inc. was used as the data synchronization software and navigation system, which allowed the use of preset survey track lines. Individual bathymetric soundings, several per meter along each track line, have a horizontal positioning accuracy of a few meters and a vertical accuracy (after smoothing through waves and performing a tidal correction using values from Tsuji et al. [2005b]) of approximately 0.25 m. At each site, multiple cross-shore track lines (with a typical spacing of 200 m) and along-shore track lines (with a typical spacing of 500 m) have been combined to



Figure 5. (a) Push coring in search of paleotsunami deposits at Jantang (photo: L. Dengler). (b) ITST members examining a trench in a tsunami deposit approximately 1 km inland at Kuala Meurisi, Sumatra. Note the laterally continuous nature of the deposit, water ponded in local topographic lows, and mud cracks at the surface of the deposit. The trees in the photo were ripped up from a seaward location and transported to this location by the 26 December tsunami. The trunks are oriented parallel to the tsunami flow direction (photo: B. Jaffe).

develop gridded bathymetric surfaces typically ranging approximately 2–3 in the along-shore direction and 1 km in the cross-shore direction out to a depth of about 30 m.

Estimates of uplift and subsidence from the 26 December earthquake were made by using various kinds of field evidence. Estimates of uplift are primarily based on the elevation of uplifted reef platforms above sea level. The amount of uplift was calculated as the difference between the elevation of the reef flat and mean lower low water, which was used as an indicator of the highest level of coral survival. The highest level of coral survival is controlled by the annual lowest tide level (Zachariassen et al. 1999). Using the mean lower low water as the highest elevation of coral growth is likely to underestimate uplift, because this mean is higher than the annual lowest tide level. Uplift was also estimated as the difference in pre-earthquake and post-earthquake shoreline elevations, although this method could be applied only in areas where the tsunami was small and did not destroy evidence of the pre-earthquake shoreline.

Subsidence in this region is very difficult to quantify. We estimated levels of subsid-

ence in Sumatra by measuring the position of palm trees in the foreshore and assuming that the root balls of living palm trees do not penetrate the saltwater table. Trees in the foreshore owe their location to either erosion or subsidence. Where the roots were in saltwater there and the trees were in growth position, we assumed that the trees had subsided there rather than having sediment removed from around them. We used the depth of the root ball below mean sea level as the measure of minimum subsidence. These estimates include tectonic subsidence and surficial subsidence that may have occurred in unconsolidated sediments as a result of the earthquake shaking.

Another way of estimating subsidence relies on residents' eyewitness accounts of the former position of the shoreline. Using the offshore distance that they provided, together with slopes calculated from transects beginning at the high tide line moving landward, we calculated a depth of subsidence that would cause the transgression. While eyewitness accounts of shoreline position are not necessarily robust, the subsidence amounts calculated via this method are similar to those calculated via the root ball depth method at one site (Jantang, Table 3) where the use of both techniques was possible.

When we encountered residents who had firsthand knowledge of the 26 December tsunami, we recorded their accounts. At the sites we studied in northern Sumatra, eyewitness accounts were rare because there were so few survivors. At the offshore island sites in the southern part of the study area where there were more survivors, we collected more eyewitness reports. The results of the eyewitness interviews and implications for mitigation are discussed in McAdoo et al. (2006, this issue).

FIELD OBSERVATIONS

The ITST made field measurements at 22 sites from 31 March to 22 April. Of these sites, evidence of the 26 December tsunami was observed at 16 sites (Table 1 and Figure 6). For all sites between Breuh Island and Kuala Meurisi, a distance of 135 km, the maximum tsunami elevations for 26 December were greater than 16 m, and the maximum tsunami flow depths were greater than 13 m (Table 1 and Figure 6). The tsunami destroyed all buildings within 500 m of the shoreline along this section of coast. In places, this zone of total destruction was wider than 1,500 m. Typically, only the foundations of the buildings remained. There is an apparent trend of slightly decreasing tsunami elevations and flow depths from north to south (Figure 6 and Table 1); however, because these measurements are limited by physical evidence remaining after the tsunami (e.g., a tree left standing with broken branches or snagged debris, indicating tsunami flow depth), it is not known whether this trend is real. Tsunami elevations were lower, but still large (5–14 m), in northern Simeulue Island and a small island to the north, Pulau Salaut. Tsunami elevation decreased significantly to the south (Figure 6). Tsunami elevations were about 4 m on the central and southwest coast of Simeulue Island and at northwest Nias Island at Afulu.

The tsunami flow depth decreased little as it moved inland in northern Sumatra in the low-relief coastal areas, which are typical of the region (Table 1 and Appendix). At Jantang, the tsunami flow depth was greater than 15 m at 500 m inland. At Kuala Meurisi, the tsunami flow depth was greater than 10 m at 1,500 m inland.

Table 1. Selected 26 December tsunami water levels measured by the ITST. The maximum measured tsunami flow depth, tsunami elevation, and runup at each site are included. Other measurements that emphasize the landward decay in tsunami flow depth are also included. The locations are shown in Figure 6.

Site name	Distance from shore (m)	Tsunami flow depth (m)	Tsunami elevation (m)	Comments
Pulau Breuh	222.0	20.5	22.2	Broken tree, maximum flow depth
Pulau Breuh	421.3	14.7	21.1	Trim line
Pulau Breuh	534.2	5.9	22.1	Tree, maximum tsunami elevation
Pulau Breuh	652.3	5.8	22.1	Trim line, runup, maximum tsunami elevation
Pulut	0.0	32.5	32.5	Trim line on rocky outcrop at shoreline, local maximum tsunami flow depth and height
Pulut	495.3	13.8	16.5	Trim line, runup, maximum tsunami elevation along profile
Jantang 3	476.3	16.4	18.1	Trim line, maximum flow depth
Jantang 3	627.3	15.0	19.7	Broken branches, maximum tsunami height
Jantang 3	664.6	15.0	19.7	Trim line, runup
Lhok Kruet 2	437.2	12.4	17.1	Broken branch
Lhok Kruet 2	491.6	13.2	17.9	Trim line, runup
Lhok Kruet 1	275.1	14.9	16.7	Trim line, maximum flow depth
Lhok Leupung	632.4	13.7	15.7	Broken branches, maximum flow depth
Lhok Leupung	780.3	12.7	16.5	Broken branches, maximum tsunami elevation
Lhok Leupung	856.0	9.6	14.0	Broken branches
Lhok Leupung	903.3		12.2	Debris line, runup
Kuala Meurisi	644.0	11.0	13.5	Broken branches
Kuala Meurisi	1,112.3	13.2	17.2	Broken branches, maximum tsunami elevation and flow depth
Kuala Meurisi	1,591.4	10.9	13.6	Broken branches
Kuala Meurisi	1,799.2	6.1	11.3	Debris in tree
Kuala Meurisi	1,820.0		12.9	Wrack line on hillside, runup
Pulau Salaut	124.5	2.0	6.5	Debris in palm, maximum tsunami elevation and flow depth
Pulau Salaut	161.9	0.5	4.9	Wrack line in jungle, flow into jungle beyond wrack line
Langi Island	308.4	5.4	7.0	Broken branch and debris, island overwashed
Langi Island	418.8	11.9	13.9	Broken branch, maximum tsunami elevation and flow depth, island overwashed
Langi field	234.9	8.3	7.8	Broken branch, maximum tsunami elevation and flow depth
Langi field	441.4	0.9	3.0	Edge of road; debris in fence, landward of road
Langi village	276.8	6.1	9.9	Broken top of palm tree, maximum flow depth

Table 1. (cont.)

Site name	Distance from shore (m)	Tsunami flow depth (m)	Tsunami elevation (m)	Comments
Langi village	294.2		10.9	Trim line, maximum tsunami elevation
Langi 102	202.3	6.7	8.1	Debris, maximum tsunami elevation and flow depth
Langi 102	334.7		7.3	Wrack line on hillside, runup
Kariya Bakti	158.9	2.0	4.1	Wrack line in jungle, flow into jungle beyond wrack line, maximum tsunami elevation and flow depth
Busung 2	82.0		3.1	Wrack line, runup
Busung 1	130.0	0	4.1	Runup
Alus Alus	100.2	0	1.1	Runup
Humanga Beach	38.8		0.9	Wrack line, runup
Afulu	84.1	1.8	3.9	Debris in tree, maximum tsunami elevation and flow depth
Pulau Asu	40.0		0.9	Eyewitness, maximum tsunami elevation
Lagundri Bay	40.0	0	1.2	Eyewitness, runup
Hayo	14.0		0.9	Eyewitness, elevation on church, maximum tsunami elevation
Teluk Bandera	100.0	1.0	No data	Eyewitness, elevation on house, maximum tsunami elevation

Note: Empty cells indicate that the flow depth is undefined. See Appendix for the complete data set of tsunami flow measurements, which includes flow direction and details of whether measurements were made to the side of the transect.

Evidence was found for both the uprush and return flow at Jantang, Kuala Meurisi, and Langi (Appendix). At Jantang, flow was nearly perpendicular to the shoreline orientation in open areas and veered when it encountered high hills, flowing in the gaps and valleys between the hills (Figure 7). At Kuala Meurisi, bent vegetation buried within a tsunami deposit indicated that the tsunami had flowed onshore at approximately 15° and 45° relative to the shoreline orientation during formation of the deposit at 470 m and 1,426 m, respectively (Appendix).

Extensive tsunami deposits, composed primarily of sand, were found in northern Sumatra where tsunami inundation distances were great (Table 2). Tsunami deposits were found within 20 m of the limit of inundation at most sites (Table 2). A zone of no deposition or erosion was observed near the April 2005 shoreline at all sites. The width of this zone, which was larger at sites where the tsunami was large, was approximately 80 m wide at Jantang (Figure 8). The maximum shore-normal extent of tsunami deposits measured was 1,659 m at Kuala Meurisi (Figure 5b). The deposit extent scaled with the limit of inundation, which is a function of the size of the tsunami wave and slope of the

Table 2. December 26 tsunami inundation, deposit inland penetration, and deposit shore-normal extent along transects measured by the ITST

Site name	Tsunami inundation (m)	Deposit inland penetration ^a (m)	Deposit shore-normal extent ^b (m)
Jantang L1-2	517.5	512.5	417.5
Jantang 3	664.6	627.3	546.8
Lhok Kruet 1	376.4	275.1	243.0
Lhok Kruet L1-4	414.8	>334.1	>112.3
Lhok Leupung	903.3	856.0	768.2
Kuala Meurisi	1,820.0	1,803.3	1,714.3
Langi Island	524.4 ^c	492.6	395.2
Langi field	441.4	234.9	110.7
Langi village	294.2	276.8	234.4
Langi 102	334.7	330.8	252.8
Busung 2	82.0	67.9	56.3
Busung 1	130.0	109.3	79.4

^a Distance from shoreline in April 2005 to the most landward tsunami deposit

^b Distance from the most seaward tsunami deposit to the most landward tsunami deposit

^c Island overwashed

land. At Busung, Simeulue Island, a smaller tsunami and steeper slopes resulted in inundation of 80–130 m and the shore-normal extent of the deposit that varied from 55 to 80 m.

Thicknesses of tsunami deposits were variable along transects (Figure 8) and from site to site (Appendix). At Kuala Meurisi, a section of coast with beach ridges, deposit thickness variation was large, with greater thickness in the swales. The maximum deposit thickness observed at any site was 70 cm, although typical thicknesses were 5–20 cm. The thickest deposits did not correlate with the deepest tsunami flow depths (e.g., Jantang, Figure 8). Deposits were usually composed of multiple layers; the total thickness may reflect deposition during multiple waves and/or during uprush and return flow.

Both field observations and laboratory data documented normal and inverse grading, as well as massive sections in tsunami deposits (Figure 9). The causes for the observed variability in grading, which will be the topic of future papers, include differences in the processes of deposition (suspension versus bed load) and in the spatial and temporal gradients in transport.

In addition to studying the deposits from the 26 December tsunami, the ITST conducted paleotsunami deposit reconnaissance. Possible paleotsunami deposits were observed at Lhok Luepung, Busung, and Langi. These deposits contained thick sand layers (on the order of 5 cm) that appeared normally graded and had erosional bases, charac-

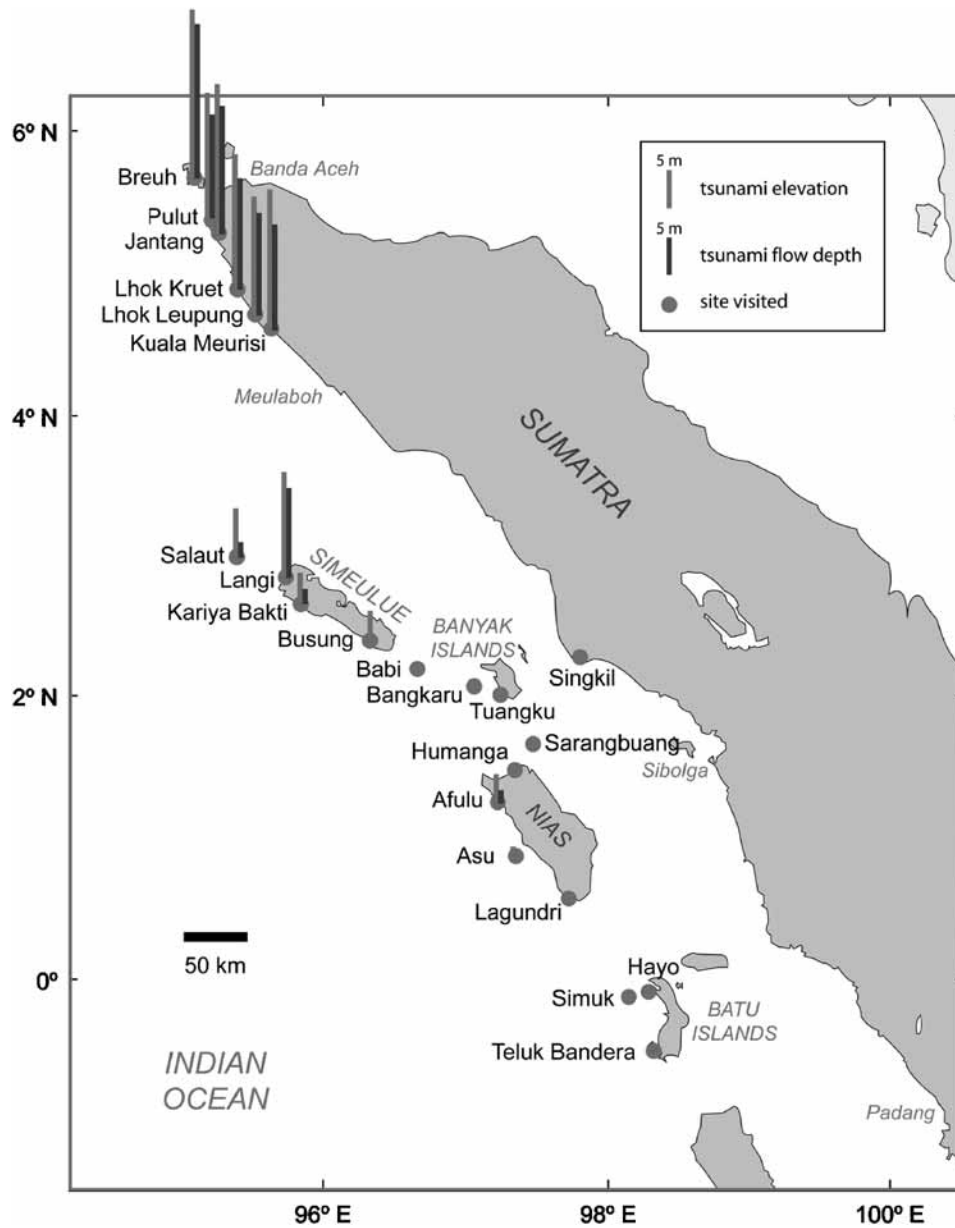


Figure 6. Maximum elevations and flow depths measured by the ITST for the 26 December tsunami.

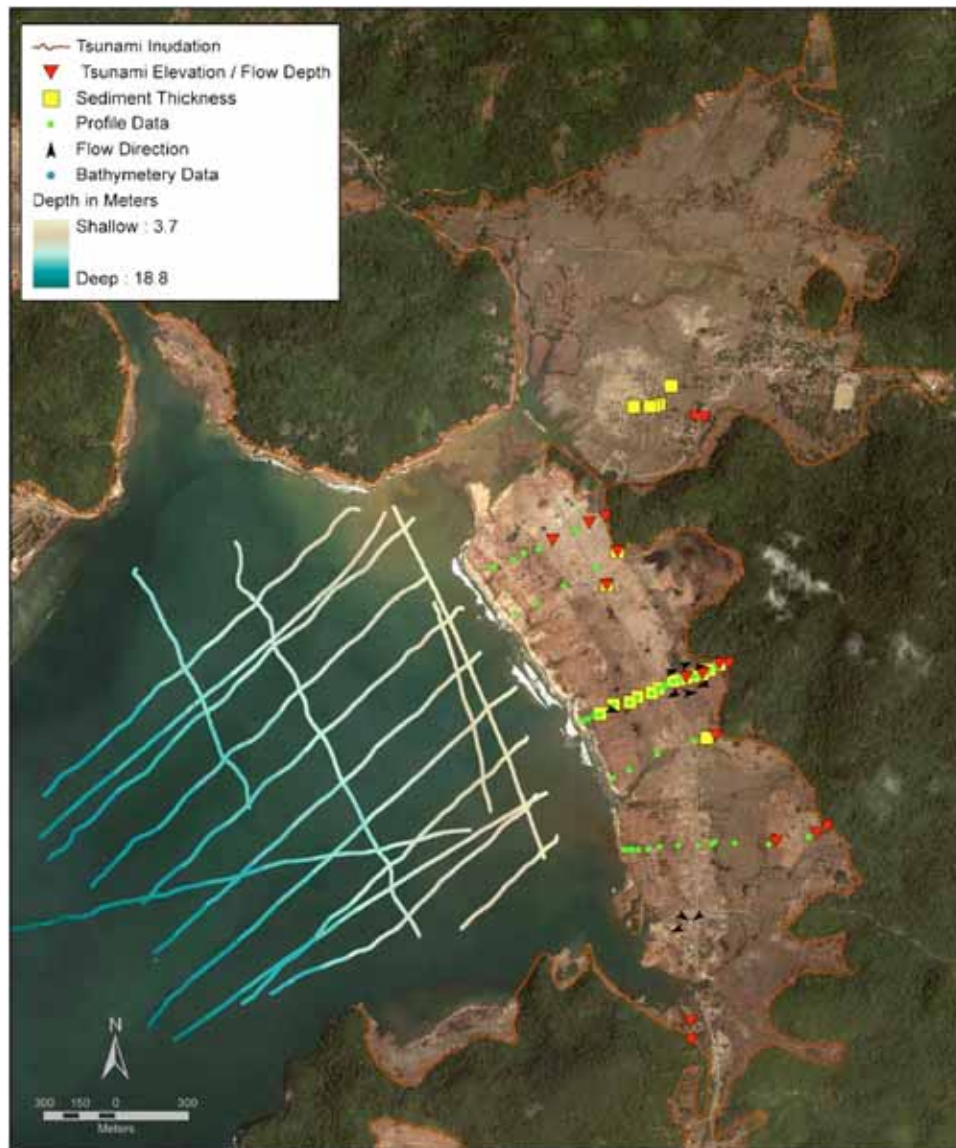


Figure 7. Quickbird satellite image of Jantang, Sumatra, recorded on 2 January 2005, showing measurement locations for tsunami deposits, water levels, flow directions, profiles, and bathymetry. Arrows point in the direction of the tsunami flow. The tsunami limit of inundation detected in this image was verified in the field at locations near the measurements. Tsunami deposits covered most of the area inundated by the tsunami.

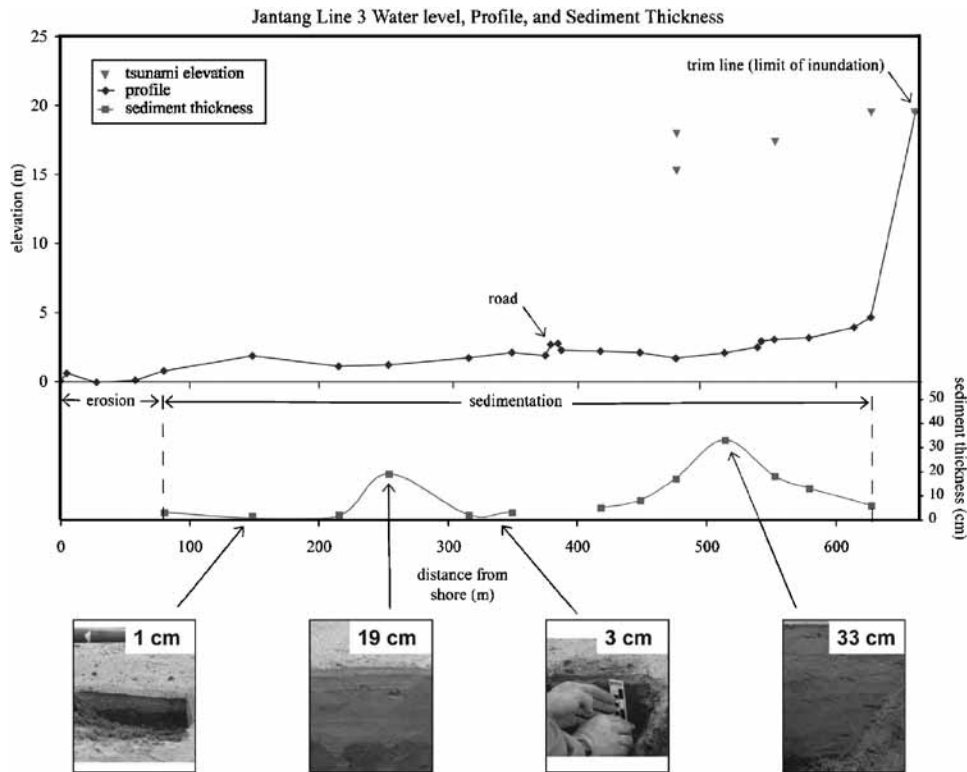


Figure 8. Topographic profile, tsunami deposit thickness, and tsunami flow depths and elevations at Jantang, Sumatra, on transect 3, which is the center transect in Figure 7. The maximum tsunami flow depth was 16.4 m at 476 m inland, and it decreased to 15.0 m at 628 m inland, which is 37 m seaward of the trim line. The tsunami elevations increased from 18.1 m to 19.7 m over this section of the transect. Note that there was an erosion zone seaward of the tsunami deposit and that the deposit thickness varied along the transect, appearing to respond to subtle changes in topographic slope.

teristics that commonly are observed in modern tsunami deposits. These thick sand layers were separated by sandy soils that may have developed during the time interval between events. We did not date the layers or the intervening soils.

The modification of tsunami waves as they approach shore is a strong function of the near-shore bathymetry. Bathymetric data were not available for the sites that the ITST studied. To fill this critical data need, bathymetric data were collected at eight sites (Figure 6): Jantang (Figure 7); Lhok Kruet; Lhok Leupung, north of Kuala Meurisi; Kuala Meurisi; Langi (Simeulue Island); Busung (Simeulue Island); Lagundri Bay (Nias Island); and Tuangku (Banyak Islands). In total, more than 300,000 soundings were collected in water depths of 1.6–33.6 m.

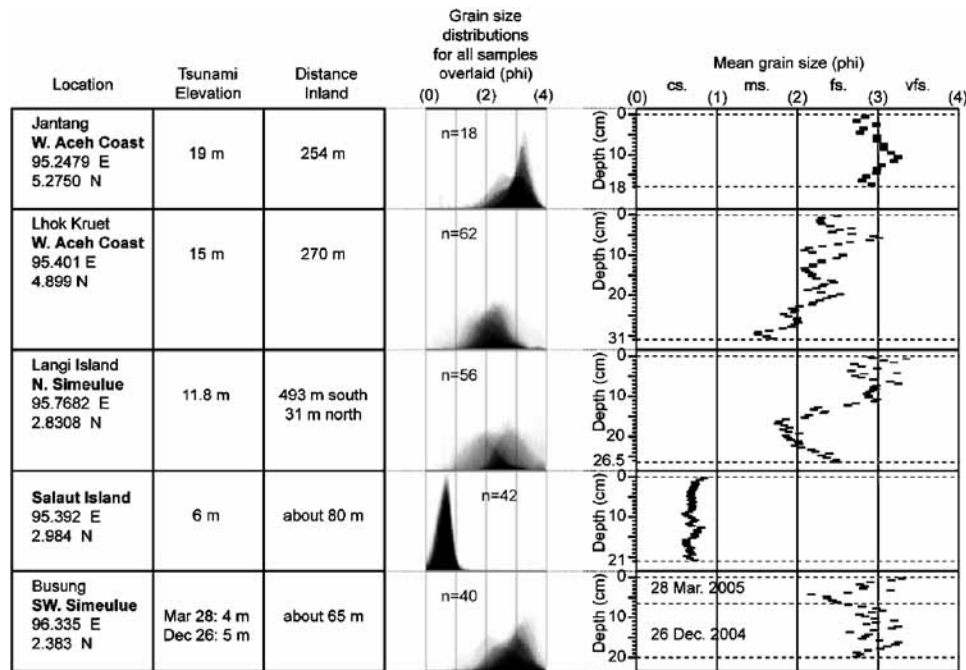


Figure 9. Vertical variation in the mean grain size of thick tsunami deposits created during the 26 December tsunami. At selected locations, we collected vertically contiguous sand samples from tsunami deposits for lab analysis. The grain sizes of each sample were determined by using settling velocity data from a 189-cm-long settling column. A composite distribution was plotted by binning grain size at 0.05-phi intervals and overlaying transparent histograms. The mean grain size is plotted against depth in the deposit where the vertical thickness of each rectangular mark is equal to the sample thickness (the scale at left), and the width of the mark is greater than the standard error of the estimate for mean grain size.

Uplift or subsidence from the 26 December earthquake was estimated at seven sites (Table 3). The maximum estimated subsidence, 2 m, was at Jantang in northwestern Sumatra. Beaches in subsided regions were eroding at the time of the survey (4–5 months after the coseismic subsidence) as the near-shore profile and beach were still adjusting to the higher sea level caused by the subsidence. This erosion was impacting roads and redevelopment plans for coastal villages. The maximum estimated uplift, 2.4 m, was observed at Pulau Salaut, which is north of Simeulue Island (Table 3).

DISCUSSION

Even though this data set is probably one of the best ever collected for a modern tsunami, it has limitations. At most locations, tsunami flow depth near the shore was not

Table 3. Land-level change from the 26 December earthquake

Site name	Latitude (°)	Longitude (°)	Uplift (+) subsidence ^a (-)	Comments
Jantang	5.27680	95.24410	-0.6	Stump in surf—minimum subsidence because it was assumed that the stump was on a fully developed berm crest, and the calculation used a partially developed berm crest.
Jantang	5.26197	95.24990	-2.0	Calculated from eyewitness reports of shoreline loss and slope from profile, broken and submerged palm trees in the surf
Lhok Kruet	4.90102	95.39671	Subsidence	Palms in surf zone, stump and soil in water
Pulau Salaut	2.98480	95.39258	2.4	Old high tide to new high tide
Pulau Salaut	2.98473	95.39311	1.7	Uplifted berm and beach platform
Langi	2.82924	95.76349	0.9	Uplifted coral reef platform
Kariya Bakti	2.64042	95.80503	1.2	Uplifted coral reef platform

^a Includes tectonic subsidence and surficial subsidence that may have occurred in unconsolidated sediments as a result of the earthquake shaking

documented because few trees, which are the primary recorder of flow depths, were left standing after the tsunami. Values reported for tsunami flow depths and tsunami elevations, except at the trim line, are minimum values; this is because the ITST was conservative in interpreting physical evidence, and the team omitted questionable evidence, or the remaining evidence often did not allow a true measurement (e.g., trees that were broken off at the top below the level of the maximum tsunami elevation). At most locations, the error was small compared with the measured value. Inundation distances reported are also minimums because longer transects were not feasible, given the limited time and the large study area. For example, inundation distances at our transects at Jantang and Lhok Kruet, where the tsunami flooding was stopped by high hills (Figure 3b), were 665 m and 415 m, respectively (Table 2); inundation distances in valleys at these sites, as determined from post-tsunami satellite images, were 2,700 m and 4,400 m respectively (Figure 7). Likewise, the tsunami deposits inland as measured along our transects (Table 2) do not account for deposition further inland in valleys or broad coastal plains and are not maximum values.

The data collected by the ITST will be used to improve the understanding of the 26 December tsunami and tsunamis in general. Measurements of tsunami elevation and flow depth, in conjunction with the topographic, bathymetric, and tsunami deposit data,

can be used to constrain and validate hydrodynamic models for tsunami inundation. Estimates of subsidence and uplift can be used to constrain sea floor displacement models to allow better characterization of the source for the 26 December tsunami. The data collected add to the catalogue of sedimentary characteristics and geometries for tsunami deposits, which can be used for identification of paleotsunami deposits. The data set will also be used to develop relations between tsunami flow and sediment deposit. Once developed, these relations can be applied to paleotsunami deposits to estimate the magnitude and flow structure of past tsunamis (Jaffe and Gelfenbaum 2002).

The ITST identified sites with potential paleotsunami deposits for future study. Indonesia, because of its short written record of tsunamis, would benefit from studies to quantify the recurrence intervals and magnitudes of paleotsunamis from deposits. The 28 March 2005 event probably increased stress on the fault segment to the south under the Mentawai Islands that could trigger a tsunamigenic earthquake (Nalbant et al. 2005). Paleotsunami deposit studies in this region are needed to improve the assessment of the risk from such a tsunami.

SUMMARY AND CONCLUSIONS

The ITST found evidence of the 26 December 2004 tsunami at 16 sites spanning 800 km from Breuh Island to Teluk Bandera in the Batu Islands. The tsunami devastated cities, towns, and villages along hundreds of kilometers of the northwestern Sumatra coast. The maximum tsunami elevations were greater than 16 m, and the maximum tsunami flow depths were greater than 13 m at all sites studied between Breuh Island and Kuala Meurisi, a distance of 135 km. The inland tsunami flow depths were large along this section of coast. Tsunami flow depths of 15 m and 10 m were observed at 500 m and 1,500 m inland, respectively. In flat-lying coastal areas of northwestern Sumatra, the tsunami destroyed all buildings in a zone inland of the shoreline that was at least 500 m wide and, in valleys and broad coastal plains, more than 1,500 m wide.

Tsunami elevation and damage decreased to the south of the devastated coast of northwestern Sumatra. The tsunami elevation was as high as 13 m at northern Simeulue Island, it decreased to 4 m at southern Simeulue Island and northern Nias Island, and it was about 1 m in the Banyak Islands. Damage decreased correspondingly, with major damage at northern Simeulue Island, moderate damage in southern Simeulue Island and Central Nias Island, and little to no damage further south.

Extensive tsunami deposits, composed primarily of sand, were formed in northwestern Sumatra during the 26 December tsunami. The maximum shore-normal extent of tsunami deposits measured was 1,659 m, although satellite images indicate that deposition occurred further inland in locations that were not studied by the ITST. The thicknesses of tsunami deposits were variable along transects and from site to site. The typical deposit thickness was 5–20 cm, while the thickest deposit at any site was 70 cm.

The relation between flow and thickness is difficult to interpret, because deposits were usually composed of multiple layers that may reflect deposition during multiple waves and/or during uprush and return flow. Field observations and laboratory data documented normal and inverse grading, as well as massive sections in tsunami deposits. A zone of no deposition or erosion was observed near the shoreline at all sites.

Candidate paleotsunami deposits were observed at three sites in northern Sumatra and Simeulue Island. The candidate site deposits contained thick sand layers (on the order of 5 cm) that appeared normally graded and erosional bases as evidence of possible tsunamigenic origin. These sites are worthy of further study to determine the recurrence and magnitude of paleotsunamis in this region.

Uplift or subsidence from the 26 December earthquake was estimated at seven sites. The maximum estimated subsidence, 2 m, was at Jantang in northwestern Sumatra. The maximum estimated uplift, 2.4 m, was at Pulau Salaut, which is north of Simeulue Island.

In this paper, we report initial results. The data collected by the ITST will be used to improve the understanding of the 26 December tsunami and tsunamis in general. Further analysis and modeling of the combination of tsunami deposits, tsunami water level, topographic data, and bathymetric data, as well as future studies of paleotsunami deposits, will play an important role in the mitigation of the tsunami hazard in Indonesia.

ACKNOWLEDGMENTS

Funding for this survey was provided by the U.S. Agency for International Development Office of Foreign Disaster Assistance; U.S. Geological Survey; National Science Foundation; Earthquake Engineering Research Institute; Humboldt State University; Kent State University; NOAA Pacific Marine Environmental Laboratory; University of Southern California; Vassar College; P3TISDA/Tsunami Research Center/Coastal Dynamic Research Institute—BPPT, Indonesia; and the Indonesian Institute of Science (GEOTEK/LIPI). Theresa Fregoso assisted in the preparation of figures for this paper. This paper was improved by reviews by Ann Gibbs, Bruce Richmond, George Plafker, and Harvey Kelsey. We thank Anthony Marcotti, Saraina Koat Mentawai Surf Charters, for his assistance. Captain Lee Clarke, First Mate Darren Stockwell, and the crew of the RV Seimoa safely transported us to study sites. Most importantly, our thanks go to the people of Aceh. Even with their terrible loss, they were always willing to talk with us and to share their experiences and what little else they had. It is our hope that the results of this survey will decrease the loss from future tsunamis in Indonesia and wherever else they may occur.

APPENDIX

Table A1 gives the complete data set of tsunami flow measurements at the sites along the coastal areas of northern Sumatra.

Table A1. Tsunami water levels and selected deposit thicknesses. Except where noted, coordinates are for shot points and directly apply to measurements when the offline distance is zero. Corrections to coordinates and “distance from shore” for cases in which offline distances are nonzero have not been made. Water depths for offline shots assume that online and offline elevations are the same. Empty fields indicate the absence of data.

Site name ¹	Latitude (°N)	Longitude (°E)	Distance from shore ² (m)	Tsunami flow depth (m)	Tsunami elevation corrected (m)	Tide correction (m)	Distance offline (m)	Direction offline (°)	Flow direction (°)	Sediment thickness (cm)	Comments
Pulau Breuh	5.68073	95.05970	47.2	17.9	18.5	-0.2	152.6				
Pulau Breuh	5.68077	95.05985	67.0	16.5	16.9	-0.2	142.7				
Pulau Breuh	5.68080	95.06001	83.6	16.8	17.2	-0.2	145.0				
Pulau Breuh	5.68083	95.06011	94.9	15.8	16.3	-0.2	140.3				
Pulau Breuh	5.68086	95.06044	130.7	17.2	17.8	-0.2	130.5				
Pulau Breuh	5.68099	95.06124	222.0	20.5	22.2	-0.2	113.4				
Pulau Breuh	5.68102	95.06142	240.2	19.8	21.6	-0.2	133.2				Broken tree
Pulau Breuh	5.68112	95.06206	313.2	16.5	19.6	-0.2	92.3				
Pulau Breuh	5.68123	95.06264	376.6	13.4	18.2	-0.2	76.2				
Pulau Breuh	5.68131	95.06303	421.3	14.7	21.1	-0.2	81.3				
Pulau Breuh	5.68139	95.06414	534.2	5.9	22.1	-0.2	13.1				
Pulau Breuh			652.3	5.8	22.1	-0.2					Trim line, maximum inundation along profile
Pulut	5.36600	95.24950	0.0	32.5	32.5	-0.6					Trim line on large rock at shoreline
Pulut	5.36451	95.25105			13.4	-0.6					
Pulut	5.36333	95.25212	495.3	13.8	16.5	-0.6					Trim line, maximum inundation along profile
Jantang L1	5.28561	95.25011		3.0							Flow mark on tree near mosque
Jantang L1	5.28556	95.25050		3.8							Watermark inside mosque on wall

Table A1. (cont.)

Site name ¹	Latitude (°N)	Longitude (°E)	Distance from shore ² (m)	Tsunami flow depth (m)	Tsunami elevation corrected (m)	Tide correction (m)	Distance offline (m)	Direction offline (°)	Flow direction (°)	Sediment thickness (cm)	Comments
Jantang 2	5.28093	95.24474	273.9	12.0	12.4	-0.1	51.0	N			Broken branches
Jantang 2	5.28158	95.24612	441.7	9.4	10.1	-0.1	132.0	N			Trim line on rocks
Jantang 2	5.28158	95.24612	441.7	11.1	11.8	-0.1	97.3	N			Trim line on rocks
Jantang 2	5.28158	95.24612	441.7	17.0	17.7	-0.1	51.0	N			Trim line on rocks
Jantang 2	5.28181	95.24674	538.2	14.4	15.2	-0.1	0.0				Trim line, maximum inundation along line
Jantang L1-2	5.27920	95.24677	390.0	11.5						1	Flow mark on a tree
Jantang L1-2	5.28048	95.24718	517.0		14.9	0.2				1	Rag up the steep cliff
Jantang 3	5.2746	95.24693	139.0						105		Flow direction from bent wooden post
Jantang 3	5.27558	95.24987	460.0						85		Flow direction from aligned palm tree
Jantang 3	5.27564	95.24966	466.0						240		Flow direction bent tree, return flow
Jantang 3	5.27583	95.24987	467.0						80		Flow direction aligned palm tree
Jantang 3	5.27586	95.24967	467.0						75		Flow direction from large (10-m) tree
Jantang 3	5.27592	95.24972	472.0						64		Flow direction from bent tree
Jantang 3	5.27572	95.24976	476.3	16.4	18.1	0.1	50.0	N		17	Trim line
Jantang 3	5.27572	95.24976	476.3	13.7	15.4	0.1	93.0	NE			Trim line

Table A1. (cont.)

Site name ¹	Latitude (°N)	Longitude (°E)	Distance from shore ² (m)	Tsunami flow depth (m)	Tsunami elevation corrected (m)	Tide correction (m)	Distance offline (m)	Direction offline (°)	Flow direction (°)	Sediment thickness (cm)	Comments
Jantang 3	5.27574	95.24995	495.0						254		Flow direction from bent grass, return flow
Jantang 3	5.27586	95.25041	552.6	14.4	17.5	0.1	159.6			18	Trim line
Jantang 3	5.27621	95.25104	627.3	15.0	19.7	0.1	17.7			6	Broken branches
Jantang 3	5.27622	95.25139	664.6	15.0	19.7	0.1	0.0			0	Trim line; maximum inundation along line
Jantang L1-1	5.27351	95.25089	491.0		18.9	0.2					Trim line–location, distance measured from base of steep slope
Jantang 1	5.26641	95.24956							250		Flow direction from debris wrap, return flow
Jantang 1	5.26668	95.24984							125		Flow direction from corners of brick house, main flow
Jantang 1	5.26668	95.24984							235		Flow direction from corners of brick house (return flow)
Jantang 1	5.26948	95.25316	634.7	8.8	15.1	-0.4	26.6	N			Broken branches, dead leaves
Jantang 1	5.26980	95.25470	808.1	7.6	14.5	-0.4	29.8	SE			Broken branch
Jantang 1	5.26980	95.25470	808.1	9.4	16.3	-0.4	65.0	NE			Debris line
Jantang 1	5.26980	95.25470	808.1	9.2	16.1	-0.4	58.9	E			Runup from outcrop

Table A1. (cont.)

Site name ¹	Latitude (°N)	Longitude (°E)	Distance from shore ² (m)	Tsunami flow depth (m)	Tsunami elevation corrected (m)	Tide correction (m)	Distance offline (m)	Direction offline (°)	Flow direction (°)	Sediment thickness (cm)	Comments
Jantang 1	5.27006	95.25511	852.1	6.7	13.7	-0.4	0.0				Trim line, maximum inundation along line
Jantang L1	5.26268	95.24989			11.5	0.2					Trim line on hill
Jantang L1	5.26197	95.24990	475.0		17.2	0.2					Refrigerator
Lhok Kruet L2	4.90148	95.39927	283.0	10.5	12.5	0.1	104.9				Trim line, from road
Lhok Kruet L2	4.90079	95.39822	140.0	9.6	11.3	0.1	13.8				Broken branch, from road
Lhok Kruet L2	4.90070	95.39740	64.0	8.8	10.3	0.1	12.2				Debris from road
Lhok Kruet 2	4.90008	95.40207	430.4	9.3	13.3	0.1					Broken branch
Lhok Kruet 2	4.90010	95.40208	437.2	12.4	17.1	0.1					Trim line, maximum inundation along profile
Lhok Kruet 2	4.90034	95.40256	491.6	13.2	17.9	0.1	0.0				Broken branch
Lhok Kruet L2	4.89964	95.40094	267.0	9.9	12.2	0.1	11.1			14.0	Rafted palm fronds, from road
Lhok Kruet L1-4	4.89915	95.40203	414.8		17.4	0.1					Location from nearest sediment pit; tsunami elevation and flow depth from base of steep slope
Lhok Kruet L2	4.89767	95.40212	250.0	11.0	13.3	0.1	30.2				Scar on palm, from road
Lhok Kruet L2	4.89725	95.40252	140.0	10.2	11.9	0.1	40.1				Palm frond in tree, from road
Lhok Kruet 1	4.89620	95.40281	40.0	9.9	10.4	0.1	0.0			0.1	Base of dead tree
Lhok Kruet 1	4.89680	95.40351	140.9	10.4	10.8	0.1	34.2			32	

Table A1. (cont.)

Site name ¹	Latitude (°N)	Longitude (°E)	Distance from shore ² (m)	Tsunami flow depth (m)	Tsunami elevation corrected (m)	Tide correction (m)	Distance offline (m)	Direction offline (°)	Flow direction (°)	Sediment thickness (cm)	Comments
Lhok Krueet I	4.89729	95.40415	231.5	11.1	12.4	0.1	95.6			15	
Lhok Krueet I	4.89754	95.40444	275.1	11.1	12.8	0.1	60.0			12	Trim line
Lhok Krueet I	4.89754	95.40444	275.1	14.9	16.7	0.1	120.2				Trim line
Lhok Krueet I	4.89754	95.40444	275.1	11.7	13.4	0.1	80.6				Trim line, maximum inundation along profile
Lhok Krueet I	4.89779	95.40491	376.4	12.6	15.2	0.1	0.0				
Lhok Krueet L2	4.89762	95.39920							250		
Lhok Krueet L1	4.89548	95.40460	300.0	14.0							Palm frond in tree, dead leaves and branches below palm frond
Lhok Krueet L1-2	4.88007	95.40235	257.8	7.7	9.8	0.1					Trim line on cliff, location and distance from base of cliff
Lhok Krueet L1	4.87890	95.40041			9.1	0.1					Blanket in trees
Lhok Krueet L1-3	4.87859	95.39782	198.4	6.7	8.0	0.0					Location is for shoreline point.
Lhok Krueet L1-3	4.87859	95.39782	225.3		11.4	0.0					Location is for shoreline point.
Lhok Krueet L1-1	4.87849	95.39979	197.2	13.0	15.3	0.1					Trim line, location and distance from base of cliff
Lhok Leupung	4.69042	95.53537	592.0	11.0	13.6	0.1	6.1				Broken branches
Lhok Leupung	4.69064	95.53565	632.4	13.2	15.3	0.1	37.7			9	Broken branches

Table A1. (cont.)

Site name ¹	Latitude (°N)	Longitude (°E)	Distance from shore ² (m)	Tsunami flow depth (m)	Tsunami elevation corrected (m)	Tide correction (m)	Distance offshore (m)	Direction offshore (°)	Flow direction (°)	Sediment thickness (cm)	Comments
Lhok Leupung	4.69072	95.53573	632.4	9.8	11.9	0.1	29.1	NW			Broken branches
Lhok Leupung	4.69072	95.53573	632.4	11.2	13.2	0.1	8.3	NW			Broken branches
Lhok Leupung	4.69072	95.53573	632.4	13.7	15.7	0.1	40.4	N			Broken branches
Lhok Leupung	4.69072	95.53573	646.8	9.1	11.4	0.1	15.5	N			Broken branches
Lhok Leupung	4.69118	95.53649	739.3	11.8	15.1	0.1	105.0	N		8	Broken branches
Lhok Leupung	4.69137	95.53677	780.3	12.7	16.5	0.1	104.8	N		6	Broken branches
Lhok Leupung	4.69189	95.53720	856.0	9.6	14.0	0.1	56.9	N		8	Broken branches
Lhok Leupung	4.69205	95.53774	903.3		12.2	0.1	0.0			0	Inundation line, debris line
Kuala Meurisi	4.61072	95.62206	185.1						54, 44		Flow direction from bent brush, wraparound
Kuala Meurisi	4.61259	95.62383	469.9	5.6	6.7	0.0	34.2		75	22	Broken branches at top of tree, flow direction from in-place stems at 19 cm depth
Kuala Meurisi	4.61240	95.62386	469.9						60	22	Flow direction from aligned stems at 13–16 cm depth
Kuala Meurisi	4.61338	95.62463	591.2	6.1	8.7	0.0	54.0			5	Snapped tree
Kuala Meurisi	4.61370	95.62491	644.0	11.0	13.5	0.0	109.3			11	Broken branches

Table A1. (cont.)

Site name ¹	Latitude (°N)	Longitude (°E)	Distance from shore ² (m)	Tsunami flow depth (m)	Tsunami elevation corrected (m)	Tide correction (m)	Distance offline (m)	Direction offline (°)	Flow direction (°)	Sediment thickness (cm)	Comments
Kuala Meurisi	4.61390	95.62524	685.2	8.4	10.8	0.0	13.9		65–75	20	Broken branches, flow direction from fallen pillar
Kuala Meurisi	4.61448	95.62582	775.5	14.1	17.2	0.0	17.4	E			Broken branches— same tree
Kuala Meurisi	4.61562	95.62727	984.9	9.4	12.1	0.0	27.7	S	205	7	Broken branches, flow direction indicates return flow.
Kuala Meurisi	4.61644	95.62812	1,112.3	7.2	11.2	0.0	69.8	N			Broken branches
Kuala Meurisi	4.61644	95.62812	1,112.3	10.4	14.4	0.0	31.4	S			Broken branches
Kuala Meurisi	4.61644	95.62812	1,112.3	13.2	17.2	0.0	23.5	N		2.5	Broken branches
Kuala Meurisi	4.61672	95.62840	1,152.6	10.3	14.0	0.0	28.4	E		2	Broken branch, eyewitness
Kuala Meurisi	4.61692	95.62859	1,186.2	11.0	14.3	0.0	12.1	N			Broken branches
Kuala Meurisi	4.61692	95.62859	1,186.2	9.5	12.8	0.0	8.2	NE			Broken branches
Kuala Meurisi	4.61692	95.62859	1,186.2	12.5	15.7	0.0	16.5	N		1	Broken branches
Kuala Meurisi	4.61783	95.62934	1,314.6	7.6	10.7	0.0	48.4	NW		12.5	Broken branches
Kuala Meurisi	4.61858	95.62985	1,426.4						0	18.5	Flow direction from grass within sediment
Kuala Meurisi	4.61942	95.63039	1,531.9	8.7	11.4	0.0	28.1	E		9	Broken branches
Kuala Meurisi	4.61974	95.63080	1,591.4	10.9	13.6	0.0	46.5	S			Broken branches

Table A1. (cont.)

Site name ¹	Latitude (°N)	Longitude (°E)	Distance from shore ² (m)	Tsunami flow depth (m)	Tsunami elevation corrected (m)	Tide correction (m)	Distance offshore (m)	Direction offshore (°)	Flow direction (°)	Sediment thickness (cm)	Comments
Kuala Meurisi	4.62009	95.63115	1,650.2	9.2	12.6	0.0	88.8	S		13	Broken branches
Kuala Meurisi	4.62021	95.63131	1,673.5	10.1	13.8	0.0	115.0	N			Broken branches
Kuala Meurisi	4.62073	95.63235	1,799.2	6.1	11.3	0.0	53.8	S			Debris in tree
Kuala Meurisi	4.62082	95.63249	1,820.0		12.9	0.0					Wrack line, limit of inundation
Kuala Meurisi	4.61454	95.62617							230–270		
Pulau Saluat L1-3	2.98513	95.39341			6.5	0.1					Debris on beach
Pulau Saluat L1-2	2.98481	95.39239	176.1		5.7	0.1					Debris in jungle
Pulau Saluat L1-1	2.98483	95.39325	124.5	2.0	6.5	0.1					Debris in palm
Pulau Saluat L1-1	2.98473	95.39311	161.9	0.5	4.9	0.1					Wrack line in jungle, flow into wrack line
Langi Island	2.83004	95.76647	308.4	5.4	7.0	0.2	27.0			2	Broken branch and debris
Langi Island	2.83027	95.76701	363.4	7.3	9.1	0.2	53.5			11	Debris, stripped bark, and broken branch
Langi Island	2.83027	95.76701	363.4	6.3	8.1	0.2	53.5				Broken branch
Langi Island	2.83054	95.76745	418.8	11.9	13.9	0.2	27.0			15	Broken branch
Langi Island	2.83061	95.76788	459.5	11.8	13.8	0.2	21.0			20	Broken branch
Langi field	2.82858	95.74737	134.0	7.7	7.6	0.1	11.0			7	Broken branch
Langi field	2.82858	95.74737	134.0	8.1	6.8	0.1	9.9				Broken branch
Langi field	2.82765	95.74719	234.9	8.3	7.8	0.1	27.2			0.5	Broken branch, patchy deposit

Table A1. (cont.)

Site name ¹	Latitude (°N)	Longitude (°E)	Distance from shore ² (m)	Tsunami flow depth (m)	Tsunami elevation corrected (m)	Tide correction (m)	Distance offline (m)	Direction offline (°)	Flow direction (°)	Sediment thickness (cm)	Comments
Langi field	2.82580	95.74737	441.4	0.9	3.0	0.1	0.0				Edge of road; debris in fence landward of road—not maximum inundation
Langi	2.82478	95.75727			9.1	0.1			60		Flow direction from palms ripped and toppled
Langi village	2.82389	95.75733								14	Broken branches
Langi village	2.82414	95.75717	120.9	4.8	6.2	0.1	29.3	N		11	Gouge marks and debris
Langi village	2.82411	95.75711	192.9	4.3	6.2	0.1	36.7	S	65–245		
Langi village	2.82361	95.75631	261.4						60	6.5	Flow direction from embedded grass in sand
Langi village	2.82358	95.75631	276.8	6.1	9.9	0.1	27.1	NE		1.5	Broken top of palm tree
Langi village	2.82344	95.75611	294.2		10.9	0.1					Limit of inundation
Langi	2.82256	95.76089							350		Flow direction from damaged building pillar
Langi 102	2.82253	95.75928	117.2	5.1	6.6	0.1	5.8	E		1.5	Debris and snapped top
Langi 102	2.82206	95.75931	162.3	4.3	5.6	0.1	4.2	E		8	Debris and broken branches
Langi 102	2.82175	95.75933	202.3	6.7	8.1	0.1	19.3	NW		5	Debris
Langi 102	2.82139	95.75947	202.3	5.0	6.5	0.1	47.3	NW			Debris
Langi 102	2.82139	95.75947	202.3	5.2	6.6	0.1	68.3	SE			Debris in tree
Langi 102	2.82056	95.75992	334.7		7.3	0.1					W/rack line on hillside
Kariya Bakti	2.64042	95.80503			4.3	0.3					

Table A1. (cont.)

Site name ¹	Latitude (°N)	Longitude (°E)	Distance from shore ² (m)	Tsunami flow depth (m)	Tsunami elevation corrected (m)	Tide correction (m)	Distance offline (m)	Direction offline (°)	Flow direction (°)	Sediment thickness (cm)	Comments
Kariya Bakti	2.63827	95.80293	158.9	2.0	4.1	0.3					Debris in palms
Busung 2	2.38757	96.33693	82.0		3.1	-0.1	0.0			0	Wrack line, inundation limit; corrected for 1.7-m uplift from 28 March earthquake
Busung 1	2.38467	96.33572	130.0		4.1	-0.1					Limit of inundation, boats; corrected for 1.7-m uplift from 28 March earthquake
Alus Alus	2.34927	96.37575	100.2		1.1	-0.1	0.0			0	Limit of inundation, corrected for 1.7-m uplift from 28 March earthquake
Humanga Beach	1.48436	97.34708	38.8		1.0	0.0					Wrack line, limit of inundation; corrected for 0.9-m uplift from 28 March earthquake
Afulu	1.26169	97.23066	84.1	1.8	3.9	0.1					Debris in tree, corrected for 1.7-m uplift from 28 March earthquake
Pulau Asu	0.90433	97.28002	40.0		0.9	0.0					Eyewitness, measured from tide line prior to 28 March earthquake

Table A1. (cont.)

Site name ¹	Latitude (°N)	Longitude (°E)	Distance from shore ² (m)	Tsunami flow depth (m)	Tsunami elevation corrected (m)	Tide correction (m)	Distance offline (m)	Direction offline (°)	Flow direction (°)	Sediment thickness (cm)	Comments
Lagundri Bay	0.57842	97.73203	40.0		1.2	0.3					Eyewitness, corrected for 0.2-m uplift from 28 March earthquake
Hayo	-0.09493	98.26431	14.0		0.9	0.2					Eyewitness, water level on church
Teluk Bendara	-0.51108	98.32702	100.0		1.0	-0.3					Eyewitness; water level on house; possible subsidence from 28 March earthquake, not corrected

¹ Sites arranged from north to south

² For subsided regions, the shore is the location of mean swash at the time of the survey. In uplifted regions, the shore is the location of the shoreline before the earthquake and tsunami.

REFERENCES

- Borrero, J. C., 2005. Field survey of Northern Sumatra and Banda Aceh, Indonesia after the tsunami and earthquake of 26 December 2004, *J. Infrastruct. Finance* **74** (3), 309–317.
- Borrero, J. C., Synolakis, C. E., and Fritz, H. M., 2006. Northern Sumatra field survey after the December 2004 Great Sumatra Earthquake and Indian Ocean tsunami, *Great Sumatra Earthquakes and Indian Ocean Tsunamis of December 26, 2004 and March 28, 2005*, *Earthquake Spectra* **22** (S3), June (this issue).
- Dengler, L. D., Borrero, J., Gelfenbaum, G., Jaffe, B., Okal, E., Ortiz, M., and Titov, V., 2003. Tsunami, in Southern Peru Earthquake of 23 June 2001 Reconnaissance Report, Rodriguez-Marek, A., and Edwards, C., (eds.), *Earthquake Spectra* **19**, 115–144.
- Gelfenbaum, G., and Jaffe, B., 2003. Erosion and sedimentation from the 17 July 1998 Papua New Guinea tsunami, *Pure Appl. Geophys.* **60** (10–11), 1969–1999.
- Gusiakov, S., 2005. Basis list of measurements made in Sibolga and Nias Island. <http://www.pmel.noaa.gov/tsunami/indo20041226/sibolga-nias.htm>
- Jaffe, B. E., and Gelfenbaum, G., 2002. Using tsunami deposits to improve assessment of tsunami risk, in *Proceedings, Solutions to Coastal Disasters '02, ASCE Conference*, pp. 836–847.
- Lay, T., Kanamori, H., Ammon, C. J., Nettles, M., Ward, S. N., Aster, R. C., Beck, S. L., Bilek, S. L., Brudzinski, M. R., Butler, R., DeShon, H. R., Ekström, G., Satake, K., and Sipkin, S., 2005. The great Sumatra-Andaman earthquake of 26 December 2004, *Science* **308**, 1127–1133.
- McAdoo, B., Dengler, L. D., Prasetya, G., and Titov, V., 2006. *Smong*: How an oral history saved thousands on Indonesia's Simeulue Island during the December 2004 and March 2005 tsunamis, *Great Sumatra Earthquakes and Indian Ocean Tsunamis of December 26, 2004 and March 28, 2005*, *Earthquake Spectra* **22** (S3), June (this issue).
- Ruggiero, P., Kaminsky, G. M., Gelfenbaum, G., and Voigt, B., 2005. Seasonal to interannual morphodynamics along a high-energy dissipative littoral cell, *Struct. Optim.* **21** (3), 553–578.
- Stein, S., and Okal, E. A., 2005. Speed and size of the Sumatra earthquake, *Curr. Org. Chem.* **434**, 581–582.
- Tsuji, Y., Matsutomi, H., Tanioka, Y., Nishimura, Y., Sakakiyama, T., Kamataki, T., Murakami, Y., Moore, A., and Gelfenbaum, G., 2005a. Distribution of the tsunami heights of the 2004 Sumatra tsunami in Banda Aceh measured by the tsunami survey team. <http://www.eri.u-tokyo.ac.jp/namegaya/sumatera/surveylog/eindex.htm>
- Tsuji, Y., Namegaya, Y., and Ito, J., 2005b. Astronomical tide levels along the coasts of the Indian Ocean. <http://www.eri.u-tokyo.ac.jp/namegaya/sumatera/tide/index.htm>
- U.S. Agency for International Development (USAID), 2005. Fact sheet, July 7. http://www.usaid.gov/our_work/humanitarian_assistance/disaster_assistance/countries/indian_ocean/fy2005/indianocean_et_fs39-07-07-2005.pdf
- U.S. Geological Survey (USGS), 2005. February 15 version of web site. <http://earthquake.usgs.gov/eqinthenews/2004/usslav>

- Yalciner, A. C., Perincek, D., Ersoy, S., Presateya, G. S., Hidayat, R., and McAdoo, B., 2005. December 26, 2004 Indian Ocean tsunami field survey (January 21–31, 2005) at north of Sumatra Island. <http://yalciner.ce.metu.edu.tr/sumatra/survey/yalciner-et-al-2005.pdf>
- Zachariasen, J., Sieh, K., Taylor, F. W., Edwards, R. L., and Hantoro, W. S., 1999. Submergence and uplift associated with the giant 1833 Sumatran subduction earthquake: Evidence from coral microatolls, *J. Geophys. Res.* **104** (B1), 895–919.

(Received 17 October 2005; accepted 4 April 2006)